

# Measurement of Light-Cone Wave Functions by Diffractive Dissociation

Daniel Ashery <sup>1</sup>

*School of Physics and Astronomy, Raymond and Beverly Sackler Faculty of Exact  
Sciences Tel Aviv University, Israel*

---

## Abstract

Diffractive dissociation of particles can be used to study their light-cone wave function. Results from Fermilab experiment E791 for diffractive dissociation of 500 GeV/c  $\pi^-$  mesons into di-jets are presented. The results show that the  $|q\bar{q}\rangle$  light-cone asymptotic wave function describes the data well for  $Q^2 \sim 10$  (GeV/c)<sup>2</sup> or more. Evidence for color transparency comes from a measurement of the  $A$ -dependence of the yield of the diffractive di-jets. It is proposed to carry out similar studies for the light-cone wave function of the photon.

---

## Introduction

### *The Pion Light-Cone Wave Function*

The internal momentum distribution of valence quarks in hadrons are fundamental to QCD. [1]. They are generated from the valence light-cone wave functions integrated over  $k_t < Q^2$ , where  $k_t$  is the intrinsic transverse momentum of the valence constituents and  $Q^2$ , the total momentum transfer squared. Even though these amplitudes were calculated about 20 years ago, there have been no direct measurements until those reported here.

The pion wave function can be expanded in terms of Fock states:

$$\Psi = a_1|q\bar{q}\rangle + a_2|q\bar{q}g\rangle + a_3|q\bar{q}gg\rangle + \dots \quad (1)$$

Two functions have been proposed to describe the momentum distribution amplitude for the quark and antiquark in the  $|q\bar{q}\rangle$  configuration. The asymptotic

---

<sup>1</sup> Supported in part by the Israel Science Foundation and the US-Israel Binational Science Foundation.

function was calculated using perturbative QCD (pQCD) methods [2–4], and is the solution to the pQCD evolution equation for very large  $Q^2$  ( $Q^2 \rightarrow \infty$ ):

$$\phi_{as}(u) = \sqrt{3}u(1-u). \quad (2)$$

$u$  is the fraction of the longitudinal momentum of the pion carried by the quark in the infinite momentum frame. It should not be confused with  $x_{Bj}$  which is not specific to a single Fock state. The antiquark carries a fraction  $(1-u)$ . Using QCD sum rules, Chernyak and Zhitnitsky [5] proposed a function that is expected to be correct for low  $Q^2$ :

$$\phi_{cz}(u) = 5\sqrt{3}u(1-u)(1-2u)^2. \quad (3)$$

As can be seen from eqns. 2 and 3 and from Fig. 1, there is a large difference between the two functions. Measurements of form factors are insensitive to the wave function as these quantities are derived by integrating over the wave function and interpretation of the results is model dependent [6]. In this work we describe an experimental study that maps the momentum distribution of the valence  $|q\bar{q}\rangle$  in the pion. This provides the first direct measurement of the pion light-cone wave function (squared). The concept of the measurement is the following: a high energy pion dissociates diffractively on a heavy nuclear target. This is a coherent process in which the quark and antiquark break apart and hadronize into two jets. If in this fragmentation process the quark momentum is transferred to the jet, measurement of the jet momentum gives the quark (and antiquark) momentum. Thus:  $u_{measured} = \frac{p_{jet1}}{p_{jet1}+p_{jet2}}$ . From simple kinematics and assuming that the masses of the jets are small compared with the mass of the di-jets, the virtuality and mass-squared of the di-jets are given by:  $Q^2 \sim M_{DJ}^2 = \frac{k_t^2}{u(1-u)}$  where  $k_t$  is the transverse momentum of each jet. By studying the momentum distribution for various  $k_t$  bins, one can observe changes in the apparent fractions of asymptotic and Chernyak-Zhitnitsky (CZ) contributions to the pion wave function.

The basic assumption that the momentum carried by the dissociating  $q\bar{q}$  is transferred to the di-jets was examined by Monte Carlo (MC) simulations of the asymptotic and (CZ) wave functions (squared). The MC samples were allowed to hadronize through the LUND PYTHIA-JETSET model [7] and then passed through simulation of the experimental apparatus (described in the next section) to simulate the effect of unmeasured neutrals and other experimental distortions. In Fig. 1 the initial distributions at the quark level are compared with the final distributions of the detected di-jets. As can be seen, the qualitative features of the distributions are retained. The results of this analysis come from comparing the observed  $u$ -distribution to a combination of the distributions shown, as examples, on the right of Figure 1.

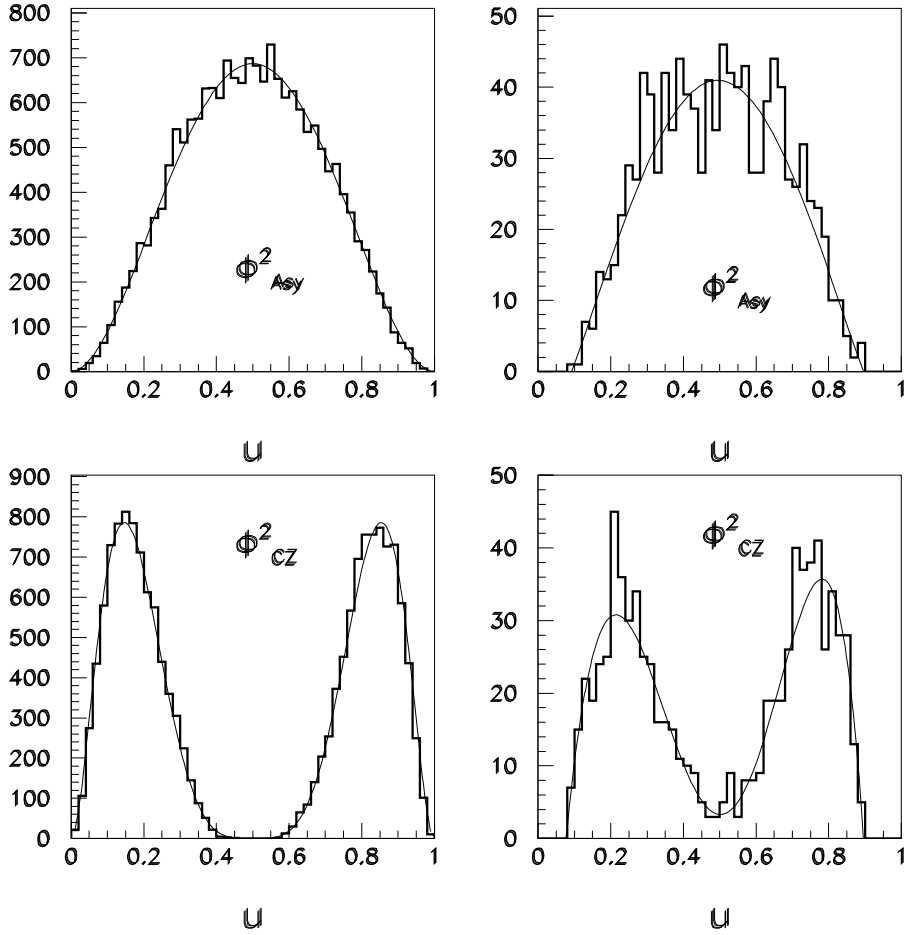


Fig. 1. Monte Carlo simulations of squares of the two wave functions at the quark level (left) and of the reconstructed distributions of di-jets as detected (right).  $\phi_{Asy}^2$  is the asymptotic function (squared) and  $\phi_{CZ}^2$  is the Chernyak-Zhitnitsky function (squared). The di-jet mass used in the simulation is  $6 \text{ GeV}/c^2$  and the plots are for  $1.5 \text{ GeV}/c \leq k_t \leq 2.5 \text{ GeV}/c$ .

### *The Color Transparency Effect*

The Color-Transparency (CT) phenomenon is derived from the prediction that color fields cancel for physically small color singlet systems of quarks and gluons [8]. This effect of color neutrality (or color screening) is expected to lead to the suppression of initial and final state interactions for a small sized system or point-like configuration (PLC) formed in a large angle hard process [9]. Observation of CT requires that a PLC is formed and that the energies are high enough so that expansion of the PLC does not occur [10] (the frozen approximation). Under conditions of  $k_t > 1.5 \text{ GeV}/c$ , which translates

to  $Q^2 \sim 10 \text{ (GeV/c)}^2$  and  $\langle r \rangle \sim 0.1 \text{ fm}$ , observation of these effects can be expected. Bertsch et al. [4] proposed that the small  $|q\bar{q}\rangle$  component will be filtered by the nucleus. Frankfurt *et al.* [11] show that for  $k_t > 1.5 \text{ GeV/c}$  the interaction with the nucleus is completely coherent and  $\sigma(|q\bar{q}\rangle N \rightarrow \text{di-jets } N)$  is small. This leads to an  $A^2$  dependence of the forward amplitude squared.

## Experimental Results

Fermilab experiment E791 recorded  $2 \times 10^{10}$  events from interactions of a  $500 \text{ GeV/c } \pi^-$  beam with carbon and platinum targets. Details of the experiment are given in [12]. Only about 10% of the E791 data was used for the analysis presented here. The data were analysed by selecting events in which 90% of the beam momentum was carried by charged particles. Jets were identified using the JADE jet-finding algorithm [13]. To insure clean selection of two-jet events, a minimum  $k_t$  of  $1.25 \text{ GeV/c}$  was required and their relative azimuthal angle, which for pure di-jets should be  $180^\circ$  was required to be within  $20^\circ$  of this value.

Diffraction di-jets were identified through the  $e^{-bq_t^2}$  dependence of their yield ( $q_t^2$  is the square of the transverse momentum transferred to the nucleus and  $b = \frac{\langle R^2 \rangle}{3}$  where  $R$  is the nuclear radius). Figure 2 shows the  $q_t^2$  distributions of di-jet events from platinum and carbon. The different slopes in the low  $q_t^2$  coherent region reflect the different nuclear radii. Events in this region come from diffractive dissociation of the pion.

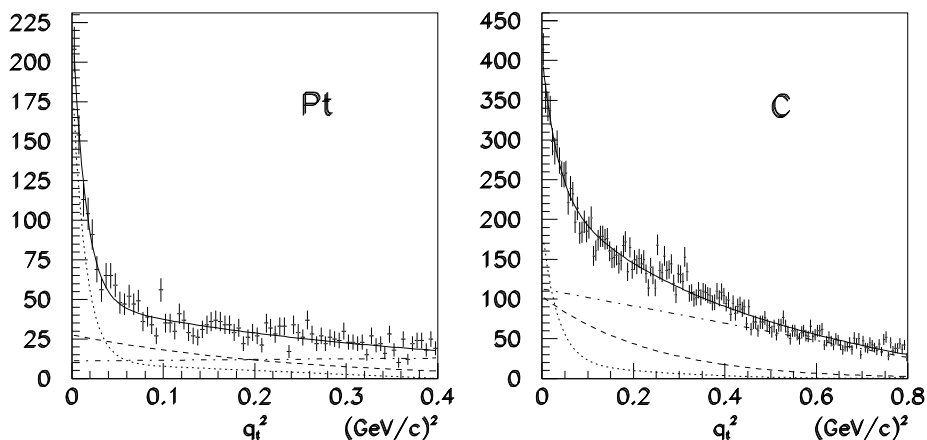


Fig. 2.  $q_t^2$  distributions of di-jets with  $1.5 \leq k_t \leq 2.0 \text{ GeV/c}$  for the platinum and carbon targets. The lines are fits of the MC simulations to the data: coherent dissociation (dotted line), incoherent dissociation (dashed line), background (dashed-dotted line), and total fit (solid line).

## The Pion Wave Function

For measurement of the wave function we used data from the platinum target as it has a sharp diffractive distribution and low background. We used events with  $q_t^2 < 0.015 \text{ GeV}/c^2$ . For these events, the value of  $u$  was computed from the measured longitudinal momentum of each jet. A background, estimated from the  $u$  distribution for events with larger  $q_t^2$  was subtracted. The analysis was carried out in two windows of  $k_t$ :  $1.25 \text{ GeV}/c \leq k_t \leq 1.5 \text{ GeV}/c$  and  $1.5 \text{ GeV}/c \leq k_t \leq 2.5 \text{ GeV}/c$ . The resulting  $u$  distributions are shown in Fig. 3. In order to get a measure of the correspondence between the experimental results and the calculated light-cone wave functions, we fit the results with a linear combination of squares of the two wave functions (right side of Fig. 1). This assumes an incoherent combination of the two wave functions and that the evolution of the CZ function is slow (as stated in [5]). The results

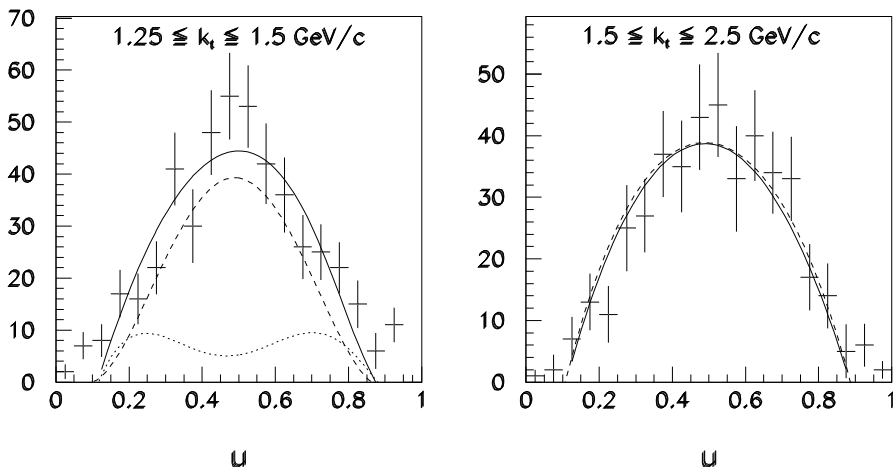


Fig. 3. The  $u$  distribution of diffractive di-jets from the platinum target for  $1.25 \leq k_t \leq 1.5 \text{ GeV}/c$  (left) and for  $1.5 \leq k_t \leq 2.5 \text{ GeV}/c$  (right). The solid line is a fit to a combination of the asymptotic and CZ wave functions. The dashed line shows the contribution from the asymptotic function and the dotted line that of the CZ function.

of the fits are given in Fig. 3 and in Table 1 in terms of the coefficients  $a_{as}$  and  $a_{cz}$  representing the contributions of the asymptotic and CZ functions, respectively. The results for the higher  $k_t$  window show that the asymptotic wave function describes the data very well. Hence, for  $k_t > 1.5 \text{ GeV}/c$ , which translates to  $Q^2 \sim 10 (\text{GeV}/c)^2$ , the pQCD approach that led to construction of the asymptotic wave function is reasonable. The distribution in the lower window is consistent with a significant contribution from the CZ wave function or may indicate contributions due to other non-perturbative effects.

$k_t$ (GeV/c)	$a_{as}$	$\Delta_{a_{as}}^{stat}$	$\Delta_{a_{as}}^{sys}$	$\Delta_{a_{as}}$	$a_{cz}$	$\Delta_{a_{cz}}^{stat}$	$\Delta_{a_{cz}}^{sys}$	$\Delta_{a_{cz}}$
1.25 - 1.5	0.64	$\pm 0.12$	+0.07 -0.01	+0.14 -0.12	0.36	$\mp 0.12$	-0.07 +0.01	-0.14 +0.12
1.5 - 2.5	1.00	$\pm 0.10$	+0.00 -0.10	+0.10 -0.14	0.00	$\mp 0.10$	-0.00 +0.10	-0.10 +0.14

Table 1

Asymptotic ( $a_{as}$ ) and CZ ( $a_{cz}$ ) wave functions contributions to a fit of the data.

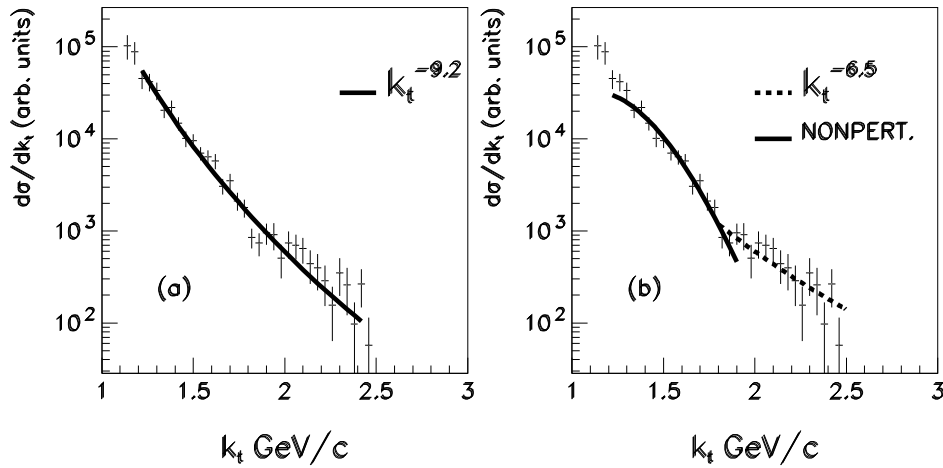


Fig. 4. Comparison of the  $k_t$  distribution of acceptance-corrected data with fits to cross section dependence (a) according to a power law, (b) based on a non-perturbative Gaussian wave function for low  $k_t$  and a power law, as expected from perturbative calculations, for high  $k_t$ .

The  $k_t$  dependence of diffractive di-jets is another observable that can show how well the perturbative calculations describe the data. As shown in [11] assuming interaction via two gluon exchange and  $\phi_{as}$  would lead to  $\frac{d\sigma}{dk_t} \sim k_t^{-6}$ . The results, corrected for experimental acceptance, are shown in figure 4(a) fitted by  $k_t^n$  for  $k_t > 1.25$  GeV with  $n = -9.2 \pm 0.4(stat) \pm 0.3(sys)$  and  $\chi^2/dof = 1.0$ . This slope is significantly larger than expected. However, the region above  $k_t \sim 1.8$  GeV/c can be fitted (Fig. 4(b)) with  $n = -6.5 \pm 2.0$  with  $\chi^2/dof = 0.8$ , consistent with the predictions. This would support the evaluation of the light-cone wave function at large  $k_t$  as due to one gluon exchange. The lower  $k_t$  region can be fitted with the non-perturbative Gaussian function:  $\psi \sim e^{-\beta k_t^2}$  [14], with  $\beta = 1.78 \pm 0.05(stat) \pm 0.1(sys)$  and  $\chi^2/dof = 1.1$ . Model-dependent values in the range of 0.9 - 4.0 were used [14]. These results are consistent with the measurements of the wave function that indicated noticeable non-perturbative effects up to  $k_t \sim 1.5$  GeV/c.

$k_t$ bin GeV/c	$\alpha$	$\Delta\alpha_{stat}$	$\Delta\alpha_{sys}$	$\Delta\alpha$	$\alpha$ (CT)
1.25 – 1.5	1.64	$\pm 0.05$	+0.04 –0.11	+0.06 –0.12	1.25
1.5 – 2.0	1.52	$\pm 0.09$	$\pm 0.08$	$\pm 0.12$	1.45
2.0 – 2.5	1.55	$\pm 0.11$	$\pm 0.12$	$\pm 0.16$	1.60

Table 2

The exponent in  $\sigma \propto A^\alpha$ , experimental results for coherent dissociation and the Color-Transparency (CT) predictions.

### *The Color Transparency Effect*

To study the CT effect we measure the A-dependence of the diffractive di-jet yield. The coherence length is estimated using  $2p_{lab} = 1000$  GeV/c and  $M_J \sim 5$  GeV/c<sup>2</sup>. The result is  $l_c \sim 10$  fm, larger than the platinum nuclear radius. In order to correct for experimental acceptance, we generate MC simulations of diffractive di-jets using the asymptotic wave function and di-jet masses of 4,5, and 6 GeV/c. The simulated coherent  $q_t^2$  distributions of the di-jets represent the nuclear form factors of carbon (R=2.44 fm) and platinum (R=5.27 fm) [15] and the incoherent dissociation is simulated according to the nucleon radius (R=0.8 fm) [15] truncated at  $q_t^2 < 0.015$ . A combination of these simulations was used to fit the data (Fig. 2). We derive the numbers of produced di-jet events in the data for each target in three  $k_t$  bins by integrating over the diffractive terms in the fits. Using the resulting yields and the known target thicknesses, we determine the ratio of cross sections for diffractive dissociation on platinum and carbon (the two targets were subjected to essentially the same beam flux). The exponents  $\alpha$  are then calculated using the cross section dependence  $\sigma \propto A^\alpha$ . The results are listed in Table 2 and compared with CT theoretical predictions [11]. The results are consistent with those expected from color-transparency calculations and clearly inconsistent with  $\alpha$  values for incoherent scattering observed in other hadronic interactions.

### **The Photon Light-Cone Wave Function**

The photon l.c. wave function can be described in a way similar to that of the pion except that it has two major components: the electromagnetic and the hadronic. Being a gauge field capable of pion-like coupling it has also a point

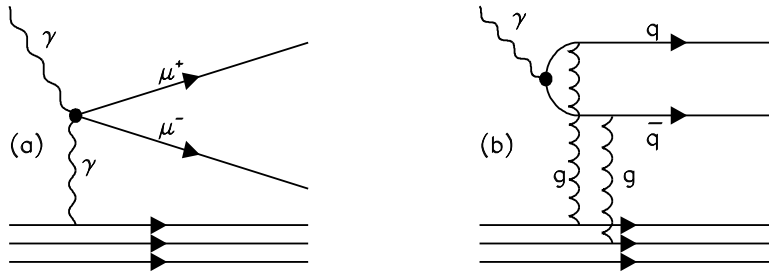


Fig. 5. Diagrams for photon dissociation

bare-photon component. Consequently, the photon light-cone wave function in the pQCD regime can be expanded in terms of Fock states:

$$\begin{aligned} \psi_\gamma = & a|\gamma_p\rangle + b|l^+l^-\rangle + c|l^+l^-\gamma\rangle + (\text{other } e.m.) \\ & + d|q\bar{q}\rangle + e|q\bar{q}g\rangle + (\text{other hadronic}) + \dots \end{aligned} \quad (4)$$

where  $|\gamma_p\rangle$  describes the point bare-photon and  $|l^+l^-\rangle$  stands for  $|e^+e^-\rangle$ ,  $|\mu^+\mu^-\rangle$  etc. The photon can be described as containing  $|q\bar{q}\rangle$  components even in the non-pQCD regime of the vector-meson dominance model [16], in particular the  $\rho$ ,  $\omega$ ,  $\phi$  and  $J/\psi$  mesons. There is also a  $|q\bar{q}\rangle$  component with large relative transverse momentum that is connected to the point-like (direct) photon. The wave function of the photon is very rich: it can be studied for real photons, for virtual photons of various virtualities, for transverse and longitudinal photons and the hadronic component may be decomposed according to the quarks flavor. Strange quarks will reflect the strange content of the photon and charmed quarks will reflect the smaller sized charmed components.

The point-bare photon does not have internal structure, it can only Compton-scatter and will not be studied here. The other electromagnetic Fock states begin with  $|l^+l^-\rangle$  and continue to more complex systems. The interaction of these Fock states with the target is expected to be purely electromagnetic, as shown in figure 5(a). These were studied extensively through measurements of Bethe-Heitler leptonproduction [17] and of  $F_{2,QED}^\gamma$  [18]. Exclusive measurements of the  $|l^+l^-\rangle$  wave function will complement these inclusive measurements, may provide more tests of QED and will help define the analysis tools for the more complex hadronic structure.

The hadronic components interact according to the diagram of Fig. 5(b). The distribution amplitudes for these components, integrated over  $k_t$  were calculated by Petrov et al. [19] using the instanton model and are shown in figure 6. Balitsky et al. [20] predict for real photons a distribution amplitude identical



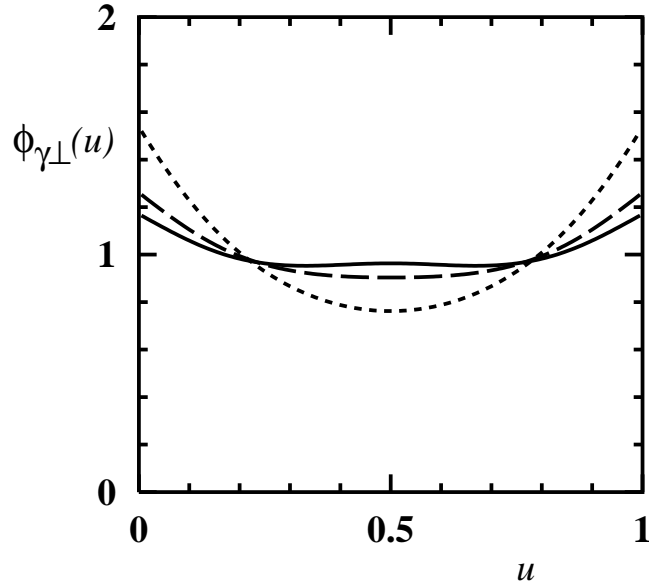


Fig. 6. The Photon wave functions, Petrov et al. Real photons (Solid line), virtual photons  $Q^2 = 250 \text{ MeV}^2$  (dashed line),  $Q^2 = 500 \text{ MeV}^2$  (dotted line).

to the pion asymptotic function [2–4] (see Fig. 1).

While a variety of cross sections, form factors etc. depend on the light-cone wave function they are usually not sensitive to its structure. This is because it normally enters the calculations in an integrated form. Such are also the photon inclusive structure functions  $F_2^\gamma$  [18]. While this is an advantage when one needs calculations that do not depend on the internal structure of the photon, it is a disadvantage if we want to understand it. A differential measurement which will be sensitive to the  $u$  and  $k_t$  dependence of  $\phi(u, Q^2)$  will test the most fundamental description of the photon internal structure. Such measurements will make it possible to compare with the theoretical predictions and determine the regime of their validity.

The experimental program is presently in preparation and is based on diffractive dissociation of a real or virtual photon into di-leptons or di-jets. The electromagnetic component will be studied through measurements of the  $u$  distribution for pure diffractive  $\mu^+\mu^-$  ( $e^+e^-$ ) elastic photoproduction and the  $k_t$  distribution of these events. Similar measurements of diffractive hadronic di-jets will be used to study the hadronic component.

I would like to acknowledge the efforts of the E791 collaboration, of which I am a member, for the data presented in this work and the data analysis performed by my graduate student R. Weiss-Babai.

## References

- [1] S.J. Brodsky, hep-ph/9908456.
- [2] S.J. Brodsky and G.P. Lepage, Phys. Rev. **D22**, 2157 (1980); S.J. Brodsky and G.P. Lepage, Phys. Scripta **23**, 945 (1981); S.J. Brodsky, Springer Tracts in Modern Physics **100**, 81 (1982).
- [3] A.V. Efremov and A.V. Radyushkin, Theor. Math. Phys. **42**, 97 (1980).
- [4] G. Bertsch, S.J. Brodsky, A.S. Goldhaber, and J. Gunion, Phys. Rev. Lett. **47**, 297 (1981).
- [5] V.L. Chernyak and A.R. Zhitnitsky, Phys. Rep. **112**, 173 (1984).
- [6] G. Sterman and P. Stoler, Ann. Rev. Nuc. Part. Sci. **43**, 193 (1997).
- [7] H.-U. Bengtsson and T. Sjöstrand, Comp. Phys. Comm. **82**, 74 (1994); T. Sjöstrand, PYTHIA 5.7 and JETSET 7.4 Physics and Manual, CERN-TH.7112/93, (1995).
- [8] F. E. Low, Phys. Rev. **D12**, 163 (1975); S. Nussinov, Phys. Rev. Lett **34**, 1286 (1975).
- [9] A.H. Mueller in Proceedings of the Seventeenth Rencontre de Moriond, Les Arcs, France (1982) ed. J. Tran Thanh Van (Editions Frontieres, Gif-sur-Yvette, France, 1982) Vol. I, p13; S.J. Brodsky in Proceedings of the Thirteenth Int'l Symposium on Multiparticle Dynamics, ed. W. Kittel, W. Metzger, and A. Stergiou (World Scientific, Singapore, 1982) p963.
- [10] S.J. Brodsky and A.H. Mueller, Phys. Lett. **B206**, 685 (1988), V.N. Gribov (1973) hep-ph/0006158, S. Mandelstam Nuovo Cim. **30**, 1148 (1963).
- [11] L.L. Frankfurt, G.A. Miller, and M. Strikman, Phys. Lett. **B304**, 1 (1993).
- [12] E791 Collaboration, E.M. Aitala *et al.*, EPJdirect **C4**, 1 (1999), S. Amato *et al.*, Nucl. Instrum. Meth. **A324** 535 (1993).
- [13] JADE collaboration, W. Bartel *et al.*, Z. Phys. **C33**, 23 (1986).
- [14] R. Jakob and P. Kroll, Phys. Lett. **B315**, 463 (1993).
- [15] Atom. Data Nucl. Data Tabl. **14**, 479 (1974).
- [16] R.P. Feynman, "Photon-Hadron Interactions", Benjamin (1972).
- [17] H.A. Bethe and W. Heitler, Proc. Royal Soc. **A146**, 85 (1934), V.B. Berestetskii, E.M. Lifshitz and L.P. Pitaevskii "Quantum Electrodynamics", Pergamon Press (1982).
- [18] R. Nisius, Phys. Rept. **332**, 165 (2000), hep-ex/9912049.
- [19] V.Yu. Petrov *et al.*, Phys.Rev. **D59**, 11401 (1999).
- [20] I.I. Balitsky *et al.*, Nucl. Phy. **B312**, 509 (1989).